Energy Levels and Lifetimes of a Two State Quantum Dot Coupled to a Ferromagnetic Lead

Bachelor thesis
Anders Jellinggaard
CPR: 210687-2395
Instructor: Karsten Flensberg

June 19, 2009

Contents

1 Synopsis *in danish*

Dette projekt omhandler en kvanteprik i forbindelse med en ferromagnetisk leder. Specifikt undersøges spinflip-hastigheder og energiniveauer op til anden orden i koblingen mellem de to komponenter.

Kvanteprikken har et enkelt spin-udartet energiniveau. Hvis begge spintilstande i niveauet er besat, frastøder de to elektroner hinanden med et potentiale U. Dette er den eneste elektron–elektron interaktion medtaget i modellen for systemet. Kvanteprikkens energiniveauer kan styres ved hjælp af et eksternt magnetfelt samt en gate-elektrode.

Lederen antages at have en spinafhængig ladningstæthed. Kombineret med gate-elektroden muliggør dette at styre spin-besætningen på kvanteprikken ved hjælp af udelukkende elektrostatiske midler, uden styring af det eksterne magnetfelt.

Størstedelen af projektet udarbejdes under fladbåndstilnærmelsen. Her antages koblingen (tilstandstætheden kombineret med transmissionskoefficienterne kvadreret) at være konstant — men spinafhængig — i et helt bånd i et metal. Båndet antages at være halvt fyldt og i termisk ligevægt.

Første ordens korrektionen til energien findes ved hjælp af pertubationsteori til at være nul. Anden ordens korrektionen til energien findes indenfor fladbåndstilnærmelsen for temperature på det absolutte nulpunkt. For et fuldstændigt kompenseret magnetfelt findes også et eksakt udtryk for energiforskellen imellem spin-op- og spin-nedtilstandene på kvanteprikken.

Udledningen af udtrykket for energiforskellen involverer indsættelsen af en infinitisimal imaginær størrelse. Det teoretiske grundlag for denne størrelse understøttes i efterfølgende kapitler, og imaginærdelen af energikorrektionen vises at være forbundet med en levetid. Dog forhindrer tilstedeværelsen af Coulomb-frastødning på kvanteprikken, at denne sammenhæng understøttes komplet.

Hastigheder for overgange væk fra de enkeltbesatte tilstande på kvanteprikken findes til første orden i koblingen ved hjælp af Fermis gyldne regel.

Til anden orden findes hastigheder for spinflip ved hjælp af en generaliseret udgave af Fermis gyldne regel inden for fladbåndstilnærmelsen. Denne udledning når ikke frem til en præcis løsning, men en tilnærmelse som er gældende hvis energiniveauerne på kvanteprikken ligger langt fra Fermi-overfladen i forhold til den termiske energi. Udledningen kræver at en endelig imaginær størrelse introduceres i T-matricen i den generaliserede gyldne regel. Denne størrelses oprindelse diskuteres kun overfladisk.

Undervejs diskuteres selvenergien for et lignende system, hvor den eneste ændring i forhold til det tidligere diskuterede system er at U er sat til nul, da dette muliggør at finde selvenergien eksakt.

2 Introduction

The electron — being a spin-$1/2$ particle — has a spin-part that can be described using only two basis states. This makes the spin of the electron one of the conceptually simplest systems in quantum mechanics,[1] and has made it an obvious candidate for the materialisation of the qubit, since its inception.[2]

The quantum dot provides an ideal platform for exploring this idea, since its large size (compared to atoms and molecules) allows for incorporation in integrated circuits,[1] while maintaining well defined energy levels. However, controlling the spin polarization of a single set of states in a quantum dot, without resorting to varying an externally applied magnetic field, has only lately been achieved.[5]

In this project, spin flip rates and energy levels are investigated up to second order in the coupling Hamiltonian. Predominantly within the context of the flat band approximation.

3 The System

A simple two component system is investigated in this project, composed of a metallic lead and a gated quantum dot. The system is located in an external magnetic field. The lead is assumed to have a spin dependant density of states. This could be caused by ferromagnetism, but the exact origin is not the focus of this project, only the effect of the density of states on the quantum dot.

The quantum dot — assumed to be in weak electrical contact with the lead — only has two states, of opposite spin but with identical spatial parts. The relative eigenenergies of the two states can be tuned by the external magnetic field.

3.1 The Hamiltonian of the system

The system described above is similar to the system used in [6], the main difference being that only one lead is considered, and the Hamiltonians are written with energies relative to the chemical potential (i.e. ξ instead of ϵ) as in [7].

We seperate the Hamiltonian in three parts — H_ℓ, H_d and $H_{\ell d}$ — corresponding to the lead, the quantum dot and the coupling, respectively, and write these partial Hamiltonians in the basis of eigenstates of $H_\ell + H_d$, i.e. with a definite number of electrons in the states of the lead and on the quantum dot.

The lead is approximated by a non-interacting Hamiltonian:

$$H_\ell = \sum_{k\sigma} \xi^\ell_{k\sigma} c^\dagger_{k\sigma} c_{k\sigma} \tag{1}$$

Note the potential spin-dependence both in the dispersion relation ($\xi^\ell_{k\sigma}$) and implicitly in the sum through a spin-dependant density of states.

The quantum dot is either occupied by nothing, one spin-up electron, one spin-down electron or both. If the dot is doubly occupied, an extra energy (U) from electrostatic repulsion is included (this term could also include contributions from electron spin-spin interactions). Lastly, we have the magnetic field $\boldsymbol{B}$, contributed to both by the external magnetic field and by the local magnetic field, caused by the adjacent ferromagnetic domain. We align the spin basis along the magnetic field, i.e. spin up is parallel to magnetic field and spin

[1] The quantum dot can be in the form of a deposited object,[3] or can be formed as part of the etching process.[4]

down is anti-parallel. The quantum dot Hamiltonian becomes

$$H_d = \xi^d \sum_\sigma d_\sigma^\dagger d_\sigma + U d_\uparrow^\dagger d_\uparrow d_\downarrow^\dagger d_\downarrow - B\frac{g_S \mu_B}{2}\left(d_\uparrow^\dagger d_\uparrow - d_\downarrow^\dagger d_\downarrow\right), \tag{2}$$

where the d's are creation and annihilation operators operating on the states of the dot, B is the magnitude of $\boldsymbol{B}$, g_s is the electron g-factor and μ_B is the Bohr magneton. The gate voltage enters ξ^d through the chemical potential. We combine the term containing the magnetic contribution to the energy with ξ^d yielding

$$\xi_\sigma^d = \xi^d - B\frac{g_S \mu_B}{2}\left(\delta_{\sigma\uparrow} - \delta_{\sigma\downarrow}\right), \tag{3}$$

such that H_d can be written as

$$H_d = \sum_\sigma \xi_\sigma^d d_\sigma^\dagger d_\sigma + U d_\uparrow^\dagger d_\uparrow d_\downarrow^\dagger d_\downarrow. \tag{4}$$

Finally a tunneling Hamiltonian couples the quantum dot to the lead:

$$H_{\ell d} = \sum_{k\sigma} T_{k\sigma} d_\sigma^\dagger c_{k\sigma} + \sum_{k\sigma} T_{k\sigma}^* c_{k\sigma}^\dagger d_\sigma. \tag{5}$$

4 Notation

This section briefly introduces the notation to be used throughout the rest of the thesis.

A complete state is denoted by

$$|\cdots\rangle_d \, |\cdots\rangle_\ell \tag{6}$$

where $|\cdots\rangle_d$ refers to the quantum dot part and $|\cdots\rangle_\ell$ refers to the lead part. The quantum dot part lives in such a small Fock space, that it becomes practical to write out all the Fock states; these are written as

$$|0\rangle_d\,,\ |\uparrow\rangle_d\,,\ |\downarrow\rangle_d \text{ and } |\uparrow\downarrow\rangle_d\,. \tag{7}$$

$|\varsigma\rangle_d$ denotes an arbitrary state from the above set, i.e. ς represents an arbitrary member of $\{0, \uparrow, \downarrow, \uparrow\downarrow\}$. Similarly $|\sigma\rangle_d$ denotes an arbitrary state in $\{|\uparrow\rangle_d\,, |\downarrow\rangle_d\}$. If σ and $\overline{\sigma}$ are used together, they refer to opposite spin.

Throughout the thesis, energy is measured in frequencies, similar to setting $\hbar$ to 1.

5 Energy Levels

We attempt to find the energy levels of the complete Hamiltonian $H = H_\ell + H_d + H_{\ell d}$ by standard perturbation theory[1] starting from the eigenstates of $H_0 = H_\ell + H_d$. However, a lot of degeneracy or near-degeneracy in H_0 makes straightforward perturbation theory difficult. Most obviously, by nature of the

direct sum, all degeneracy in the lead taken alone is carried over into the composite states. I.e. for all sets of lead states (A) that were degenerate with respect to H_ℓ there will be a degenerate subspaces of the form

$$\{|\varsigma\rangle_d |a\rangle_\ell : |a\rangle_\ell \in A\} \tag{8}$$

for each ς in $\{0, \uparrow, \downarrow, \uparrow\downarrow\}$. However this does not pose a problem, since these subspaces are diagonal in $H_{\ell d}$, as can easily be seen by looking at the possible matrix elements. We have

$$\begin{aligned}\langle a|_\ell \langle \varsigma|_d H_{\ell d} |\varsigma\rangle_d |b\rangle_\ell = &\sum_{k\sigma} T_{k\sigma} \overbrace{\langle \varsigma|_d d_\sigma^\dagger |\varsigma\rangle_d}^{\text{This is zero}} \langle a|_\ell c_{k\sigma} |b\rangle_\ell \\ &+ \sum_{k\sigma} T_{k\sigma}^* \langle a|_\ell c_{k\sigma}^\dagger |b\rangle_\ell \underbrace{\langle \varsigma|_d d_\sigma |\varsigma\rangle_d}_{\text{So is this}}\end{aligned} \tag{9}$$

which is zero (incidentally, all the elements of the main diagonal are zero too).

The problematic degeneracy occurs when one electron has been moved from the lead to the quantum dot or vice versa, while maintaining the total energy. E.g. the following two expressions (and the two expression with the states interchanged) represent off-diagonal elements between degenerate states (provided that $|a\rangle_\ell$ is empty in the $k\sigma$-state):

$$\langle a|_\ell \langle \sigma|_d H_{\ell d} |0\rangle_d c_{k\sigma}^\dagger |a\rangle_\ell = T_{k\sigma} \tag{10}$$

where the states are degenerate if $\xi_{k\sigma}^\ell$ equals ξ_σ^d, and

$$\langle a|_\ell \langle \uparrow\downarrow|_d H_{\ell d} |\overline{\sigma}\rangle_d c_{k\sigma}^\dagger |a\rangle_\ell = T_{k\sigma} \tag{11}$$

where the states are degenerate if $\xi_{k\sigma}^\ell$ equals $\xi_\sigma^d + U$.

Since we do not know in general what the $T_{k\sigma}$'s are, there is no easy way to move on from here. We ignore this potential disaster for now and continue using non-degenerate perturbation theory.

The first order corrections to the energy of all states are zero, as has in fact already been covered by equation (9). We now turn to the second order correction of an arbitrary Fock state $|\sigma\rangle_d |a\rangle_\ell$ with σ in $\{\uparrow, \downarrow\}$, given as

$$E_{a\sigma}^{(2)} = \sum_{b\varsigma} \frac{|\langle b|_\ell \langle \varsigma|_d H_{\ell d} |\sigma\rangle_d |a\rangle_\ell|^2}{E_{a\sigma}^{(0)} - E_{b\varsigma}^{(0)}}, \tag{12}$$

where the sum runs over all Fock states excluding the one indexed by a and σ, and $E_{b\varsigma}^{(0)}$ is the eigenenergy of $|\varsigma\rangle_d |b\rangle_\ell$ with respect to H_0.

Inserting the expression for $H_{\ell d}$ dramatically reduces the amount of states to be summed over, as the numerator is only non-zero for states that can be

reached from $|\sigma\rangle_d |a\rangle_\ell$ by moving a single electron. We have

$$\begin{aligned} E^{(2)}_{a\sigma} &= \sum_{\boldsymbol{k}} \frac{\left|\langle a|_\ell \, c^\dagger_{\boldsymbol{k}\bar{\sigma}} \langle\sigma|_d \, d_{\bar{\sigma}} \; T_{\boldsymbol{k}\bar{\sigma}} d^\dagger_{\bar{\sigma}} c_{\boldsymbol{k}\bar{\sigma}} |\sigma\rangle_d |a\rangle_\ell\right|^2}{\xi^\ell_{\boldsymbol{k}\bar{\sigma}} - \xi^d_{\bar{\sigma}} - U} \\ &\quad + \sum_{\boldsymbol{k}} \frac{\left|\langle a|_\ell \, c_{\boldsymbol{k}\sigma} \langle\sigma|_d \, d^\dagger_\sigma \; T^*_{\boldsymbol{k}\sigma} c^\dagger_{\boldsymbol{k}\sigma} d_\sigma |\sigma\rangle_d |a\rangle_\ell\right|^2}{-\xi^\ell_{\boldsymbol{k}\sigma} + \xi^d_\sigma} \\ &= \sum_{\boldsymbol{k}} \frac{|T_{\boldsymbol{k}\bar{\sigma}}|^2 \left|\langle a|_\ell \langle\sigma|_d \, c^\dagger_{\boldsymbol{k}\bar{\sigma}} c_{\boldsymbol{k}\bar{\sigma}} (1 - d^\dagger_{\bar{\sigma}} d_{\bar{\sigma}}) |\sigma\rangle_d |a\rangle_\ell\right|^2}{\xi^\ell_{\boldsymbol{k}\bar{\sigma}} - \xi^d_{\bar{\sigma}} - U} \\ &\quad + \sum_{\boldsymbol{k}} \frac{|T_{\boldsymbol{k}\sigma}|^2 \left|\langle a|_\ell \langle\sigma|_d \, (1 - c^\dagger_{\boldsymbol{k}\sigma} c_{\boldsymbol{k}\sigma}) d^\dagger_\sigma d_\sigma |\sigma\rangle_d |a\rangle_\ell\right|^2}{-\xi^\ell_{\boldsymbol{k}\sigma} + \xi^d_\sigma}. \end{aligned} \tag{13}$$

The quantum dot occupation number operators $d^\dagger_{\bar{\sigma}} d_{\bar{\sigma}}$ and $d^\dagger_\sigma d_\sigma$ above evaluates to 0 and $|\sigma\rangle_d$ respectively, when operating on $|\sigma\rangle_d$. Furthermore, since the states in the numerator are Fock states, they have exactly zero or one electron in each state by definition. Therefore, each inner product in the numerator must either yield 0 or 1, and we may as well drop the $|\cdots|^2$. The expression above can thus be simplified to

$$\begin{aligned} E^{(2)}_{a\sigma} &= \sum_{\boldsymbol{k}} \frac{|T_{\boldsymbol{k}\bar{\sigma}}|^2 \langle a|_\ell \langle\sigma|_d \, c^\dagger_{\boldsymbol{k}\bar{\sigma}} c_{\boldsymbol{k}\bar{\sigma}} |\sigma\rangle_d |a\rangle_\ell}{\xi^\ell_{\boldsymbol{k}\bar{\sigma}} - \xi^d_{\bar{\sigma}} - U} \\ &\quad + \sum_{\boldsymbol{k}} \frac{|T_{\boldsymbol{k}\sigma}|^2 \langle a|_\ell \langle\sigma|_d \, (1 - c^\dagger_{\boldsymbol{k}\sigma} c_{\boldsymbol{k}\sigma}) |\sigma\rangle_d |a\rangle_\ell}{-\xi^\ell_{\boldsymbol{k}\sigma} + \xi^d_\sigma}. \end{aligned} \tag{14}$$

Finally, since the occupation numbers of the lead states are independent of the quantum dot parts, we can save some ink by writing

$$E^{(2)}_{a\sigma} = \sum_{\boldsymbol{k}} \frac{|T_{\boldsymbol{k}\bar{\sigma}}|^2 \langle a|_\ell \, c^\dagger_{\boldsymbol{k}\bar{\sigma}} c_{\boldsymbol{k}\bar{\sigma}} |a\rangle_\ell}{\xi^\ell_{\boldsymbol{k}\bar{\sigma}} - \xi^d_{\bar{\sigma}} - U} + \sum_{\boldsymbol{k}} \frac{|T_{\boldsymbol{k}\sigma}|^2 \langle a|_\ell \, (1 - c^\dagger_{\boldsymbol{k}\sigma} c_{\boldsymbol{k}\sigma}) |a\rangle_\ell}{-\xi^\ell_{\boldsymbol{k}\sigma} + \xi^d_\sigma}. \tag{15}$$

More interesting than the energy-correction to a specific combination of lead and quantum dot states (which is immaterial, since we cannot know the state of the lead exactly) is the thermal average of the possible $|a\rangle_\ell$ states, with only the quantum dot part known. We approximate this using the thermal average with respect to H_0, using a definition similar to the normal definition[7]. However, the sums here runs over only the eigenstates of H_0 that have a quantum dot part of exactly $|\sigma\rangle_d$.[2] I.e.

$$E^{(2)}_\sigma \equiv \frac{\sum_a e^{-\beta E^{(0)}_{a\sigma}} E^{(2)}_{a\sigma}}{\sum_a e^{-\beta E^{(0)}_{a\sigma}}} = \frac{\sum_a e^{-\beta(E^\ell_a + \xi^d_\sigma)} E^{(2)}_{a\sigma}}{\sum_a e^{-\beta(E^\ell_a + \xi^d_\sigma)}} = \frac{\sum_a e^{-\beta E^\ell_a} E^{(2)}_{a\sigma}}{\sum_a e^{-\beta E^\ell_a}}, \tag{16}$$

where β equals $1/k_B T$ and E^ℓ_a is the energy of $|a\rangle_\ell$ with respect to H_ℓ.

[2] This would have been problematic if the thermal average was with respect to the full Hamiltonian, since states with a known quantum dot part are not eigenvalues of H and hence have ill-defined energies.[7]

We move the sum over a into the sum over $\boldsymbol{k}$, obtaining

$$E_\sigma^{(2)} = \sum_{\boldsymbol{k}} \frac{|T_{\boldsymbol{k}\bar{\sigma}}|^2 \frac{\sum_a e^{-\beta E_a^\ell} \langle a|_\ell c_{\boldsymbol{k}\bar{\sigma}}^\dagger c_{\boldsymbol{k}\bar{\sigma}} |a\rangle_\ell}{\sum_a e^{-\beta E_a^\ell}}}{\xi_{\boldsymbol{k}\bar{\sigma}}^\ell - \xi_{\bar{\sigma}}^d - U} + \sum_{\boldsymbol{k}} \frac{|T_{\boldsymbol{k}\sigma}|^2 \frac{\sum_a e^{-\beta E_a^\ell} \langle a|_\ell (1 - c_{\boldsymbol{k}\sigma}^\dagger c_{\boldsymbol{k}\sigma}) |a\rangle_\ell}{\sum_a e^{-\beta E_a^\ell}}}{-\xi_{\boldsymbol{k}\sigma}^\ell + \xi_\sigma^d}$$

$$= \sum_{\boldsymbol{k}} \frac{|T_{\boldsymbol{k}\bar{\sigma}}|^2 n_F(\xi_{\boldsymbol{k}\bar{\sigma}}^\ell)}{\xi_{\boldsymbol{k}\bar{\sigma}}^\ell - \xi_{\bar{\sigma}}^d - U} + \sum_{\boldsymbol{k}} \frac{|T_{\boldsymbol{k}\sigma}|^2 \left(1 - n_F(\xi_{\boldsymbol{k}\sigma}^\ell)\right)}{-\xi_{\boldsymbol{k}\sigma}^\ell + \xi_\sigma^d}, \tag{17}$$

where n_F is the Fermi-Dirac distribution (see section A.1 for a derivation of the Fermi-Dirac distribution from the sums above).

5.1 Flat band

In the hopes of discovering some of the qualitative features of equation (17) we turn to a particularly simple combination of $\xi_{\boldsymbol{k}\sigma}^\ell$ and density of states: The flat band[6].

The relation between the wave vector $\boldsymbol{k}$ and $\xi_{\boldsymbol{k}\sigma}^\ell$ can in general be anisotropic and non-bijective,[8] making it generally impossible to deduce $T_{\boldsymbol{k}\sigma}$ from $\xi_{\boldsymbol{k}\sigma}^\ell$ alone. But assuming that we can at least approximate this function (for example if both depends on the length of $\boldsymbol{k}$ in a simple way[7]), it becomes possible to convert the sums in (17) to simple integrals given by[3]

$$E_\sigma^{(2)} = \int_\xi \mathcal{D}_{\bar{\sigma}}(\xi) \frac{|T_{\bar{\sigma}}(\xi)|^2 n_F(\xi)}{\xi - \xi_{\bar{\sigma}}^d - U} d\xi + \int_\xi \mathcal{D}_\sigma(\xi) \frac{|T_\sigma(\xi)|^2 (1 - n_F(\xi))}{-\xi + \xi_\sigma^d} d\xi, \tag{18}$$

where $\mathcal{D}_\sigma(\xi)$ represents the density of states and $T_\sigma(\xi)$ is $T_{\boldsymbol{k}\sigma}$ as a function of $\xi_{\boldsymbol{k}\sigma}^\ell$. Defining the coupling[6]

$$\Gamma_\sigma(\xi) \equiv \pi \mathcal{D}_\sigma(\xi) |T_\sigma(\xi)|^2, \tag{19}$$

this can be written as

$$E_\sigma^{(2)} = \tfrac{1}{\pi} \int_\xi \Gamma_{\bar{\sigma}}(\xi) \frac{n_F(\xi)}{\xi - \xi_{\bar{\sigma}}^d - U} d\xi + \tfrac{1}{\pi} \int_\xi \Gamma_\sigma(\xi) \frac{1 - n_F(\xi)}{-\xi + \xi_\sigma^d} d\xi. \tag{20}$$

If the metal constituting the lead has an odd valence (i.e. it is not a semimetal), the conduction band will be approximately half-full.[8] This information is encoded in the density of states being 0 for ξ outside an interval $[-D, D]$. Inside the interval, the coupling is approximated by a (spin-dependant) constant.[7]

$$\Gamma_\sigma(\xi) = \begin{cases} \Gamma_\sigma & \text{if } |\xi| < D \\ 0 & \text{otherwise.} \end{cases} \tag{21}$$

With these approximations, the integrals in (20) can be written as

$$E_\sigma^{(2)} = \tfrac{1}{\pi} \int_{-D}^{D} \Gamma_{\bar{\sigma}} \frac{n_F(\xi)}{\xi - \xi_{\bar{\sigma}}^d - U} d\xi + \tfrac{1}{\pi} \int_{-D}^{D} \Gamma_\sigma \frac{1 - n_F(\xi)}{-\xi + \xi_\sigma^d} d\xi. \tag{22}$$

[3] see [7] for a similar calculation in the context of the Anderson model for magnetic impurities

5.1.1 At absolute zero

At absolute zero, the Fermi-Dirac distribution functions in (22) becomes step-functions, completely cutting of the upper part of the first integral and the lower part of the second. I.e.

$$E_\sigma^{(2)} = \tfrac{1}{\pi}\int_{-D}^{0} \frac{\Gamma_{\overline{\sigma}}}{\xi - \xi_{\overline{\sigma}}^{d} - U} d\xi + \tfrac{1}{\pi}\int_{0}^{D} \frac{\Gamma_\sigma}{-\xi + \xi_\sigma^{d}} d\xi. \tag{23}$$

If we avoid the poles by only looking at situations where $\xi_{\overline{\sigma}}^{d} + U > 0$ and $\xi_\sigma^{d} < 0$, the integrals become proper integrals[4] with the solution

$$E_\sigma^{(2)} = \frac{\Gamma_{\overline{\sigma}}}{\pi}\log\left(\frac{\xi_{\overline{\sigma}}^{d} + U}{D + \xi_{\overline{\sigma}}^{d} + U}\right) + \frac{\Gamma_\sigma}{\pi}\log\left(\frac{-\xi_\sigma^{d}}{D - \xi_\sigma^{d}}\right). \tag{24}$$

When the half-width of the band (D) is large compared to $\left|\xi_\sigma^{d}\right|$, $\left|\xi_{\overline{\sigma}}^{d}\right|$ and U, which it is in at least one experimental realization,[5] this expression is well approximated by

$$E_\sigma^{(2)} = \frac{\Gamma_{\overline{\sigma}}}{\pi}\log\left(\frac{\xi_{\overline{\sigma}}^{d} + U}{D}\right) + \frac{\Gamma_\sigma}{\pi}\log\left(\frac{-\xi_\sigma^{d}}{D}\right). \tag{25}$$

Written in this form, it is clear that the difference between the energy correction of $|\uparrow\rangle_d$ and $|\downarrow\rangle_d$ can be expressed without D. The difference is given as

$$\Delta E^{(2)} \equiv E_\uparrow^{(2)} - E_\downarrow^{(2)} = \frac{\Gamma_\uparrow}{\pi}\log\left(\frac{-\xi_\uparrow^{d}}{\xi_\uparrow^{d} + U}\right) - \frac{\Gamma_\downarrow}{\pi}\log\left(\frac{-\xi_\downarrow^{d}}{\xi_\downarrow^{d} + U}\right). \tag{26}$$

See figure 1 for a visualization of $\Delta E^{(2)}$. We see from this figure that the effect of the gate voltage on the spin population is most pronounced when $\xi_\uparrow^{d}$ equals $\xi_\downarrow^{d}$. This requires that the external magnetic field cancels the local magnetic field, which can only happen if the two are aligned.

In this case

$$\Delta E^{(2)} = \frac{\Delta\Gamma}{\pi}\log\left(\frac{-\xi^{d}}{\xi^{d} + U}\right) \tag{27}$$

where $\Delta\Gamma$ equals $\Gamma_\uparrow - \Gamma_\downarrow$ and $\xi^{d} = \xi_\uparrow^{d} = \xi_\downarrow^{d}$. This expression is given in [6]. The sign of $\Delta E^{(2)}$, and thus the spin of the most favourable state, is decided by the ratio

$$\frac{-\xi^{d}}{\xi^{d} + U}. \tag{28}$$

If $\Delta\Gamma$ is positive, and the above ratio is below one, the favourable state on the quantum dot is the spin up state. This is caused by increased hybridization

[4] Technically, the integrands still have singularities at the poles, even if they fall where the distributions yield zero. But these singularities are removable when the temperature is zero.

[5] Compare the width of the diamonds in figure 1 in [5] with the band structure of nickel[9].

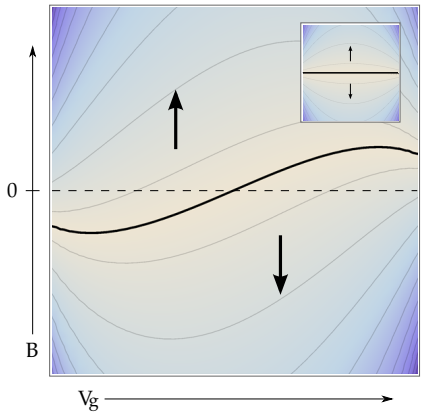

Figure 1: *This figure shows the energy difference between $|\uparrow\rangle_d$ and $|\downarrow\rangle_d$ for the flat band, found by second order perturbation theory at* 0 °K *(see section 5.1).*
The x and y parameters are the gate voltage and the magnetic field respectively. In contrast to the rest of the thesis, the spin-basis here is fixed, and the magnetic field is varied in relation to it, allowing the effect of reversing the magnetic field to be displayed in one plot. The magnetic field is parallel or anti-parallel to spin up, with the component plotted along the y-axis as B.
Darker shading represents higher absolute energy difference. Arrows represent the spin of the lowest energy state in each region. In effect, the arrows reflect the sign of the energy difference. $\xi^d_\uparrow$ equals $\xi^d_\downarrow$ in the vertical center of the plot.
In the main graphic $\Gamma_\uparrow$ is slightly smaller than $\Gamma_\downarrow$, whereas they are the same in the small embedded graphic (corresponding to a lead that is not ferromagnetic).

as the singly-occupied quantum dot state approaches the empty lead-states above the Fermi level. The virtual process corresponding to this hybridization is fluctuations off and then onto the quantum dot, with an intermittent empty quantum dot.

When the ratio is higher than one, in which case $\xi^d + U$ is closest to the Fermi level, the spin down state is favoured. As this allows spin up lead-states to hybridize onto the quantum dots empty spin up state. The virtual process in this case, corresponds to spin up electrons in the lead, fluctuating between the spin up state on the quantum dot and the lead. In this case, the quantum dot is intermittently doubly occupied. Both situations are shown in figure 2.

The transition point lies at

$$\xi^d = -\frac{U}{2}, \tag{29}$$

which corresponds to the Fermi level being positioned halfway between the singly-occupied and doubly-occupied energy levels.

5.1.2 At finite temperatures

Using lessons learned from the zero temperature case, we now take another stab at (22), this time without resorting to setting T equals zero.

Since the energy correction diverges for D much greater than the three characteristic energies of the quantum dot ($\xi^d_\uparrow$, $\xi^d_\downarrow$ and U), we again choose to look at only the *difference* between the energy corrections of the two single

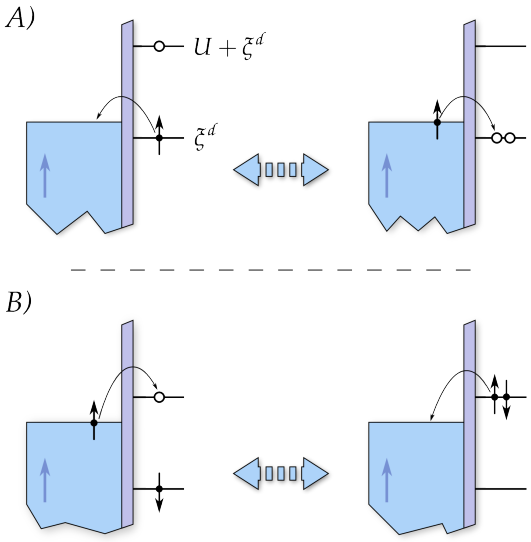

Figure 2: *This figure depicts the virtual processes which leads to the perturbed energy levels. $\Delta\Gamma$ is positive in both A) and B), signifying a majority of spin up states on the lead.*
For $|\xi^d| < |\xi^d + U|$, the larger coupling of the spin up state on the quantum dot with empty lead states near the Fermi level, causes this level to be lower in energy than the corresponding spin down state. This is depicted in A).
In B), the gate potential has been tuned such that $|\xi^d| > |\xi^d + U|$. In this case the spin down state is favoured, as this leaves the spin up state of the dot available for hybridization with the spin up electrons in the lead.
This figure is an adaptation of a figure in [5].

particle quantum dot states. At finite temperatures this reads as

$$\Delta E^{(2)} = \tfrac{1}{\pi}\int_{-D}^{D}\left(\Gamma_\downarrow \frac{n_F(\xi)}{\xi - \xi^d_\downarrow - U} + \Gamma_\uparrow \frac{1-n_F(\xi)}{-\xi + \xi^d_\uparrow} - \Gamma_\uparrow \frac{n_F(\xi)}{\xi - \xi^d_\uparrow - U} - \Gamma_\downarrow \frac{1-n_F(\xi)}{-\xi + \xi^d_\downarrow}\right) d\xi. \tag{30}$$

Similar to (27), we employ the restriction $\xi^d_\uparrow = \xi^d_\downarrow$ and express $\Delta E^{(2)}$ using the coupling difference ($\Delta\Gamma$) as

$$\begin{aligned}\Delta E^{(2)} &= -\frac{\Delta\Gamma}{\pi}\int_{-D}^{D}\left(\frac{n_F(\xi)}{\xi - \xi^d - U} + \frac{1-n_F(\xi)}{\xi - \xi^d}\right) d\xi \\ &= -\frac{\Delta\Gamma}{\pi}\int_{-D}^{D}\left(\frac{1}{e^{\beta\xi}+1}\,\frac{1}{\xi - \xi^d - U} + \frac{1}{e^{-\beta\xi}+1}\,\frac{1}{\xi - \xi^d}\right) d\xi.\end{aligned} \tag{31}$$

Using the substitution $z = \beta\xi$, the integral simplifies to

$$\Delta E^{(2)} = -\frac{\Delta\Gamma}{\pi}\int_{-\beta D}^{\beta D}\left(\frac{1}{e^{z}+1}\,\frac{1}{z - a} + \frac{1}{e^{-z}+1}\,\frac{1}{z - b}\right) dz, \tag{32}$$

where $a = \beta(\xi^d + U)$ and $b = \beta\xi^d$. Our strategy is to solve this integral for $\beta D \to \infty$ using contour integration.

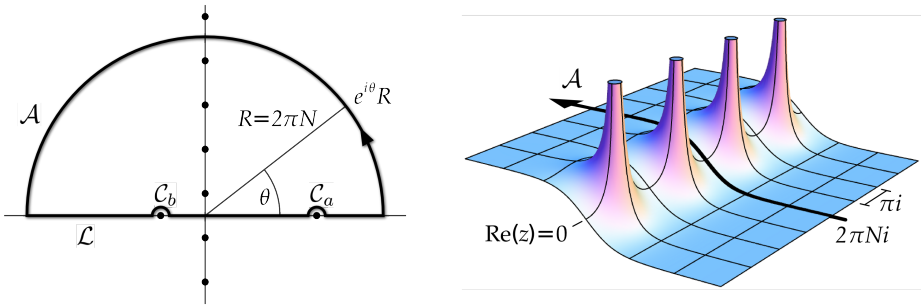

Figure 3: *On the left, the contour used to calculate $\Delta E^{(2)}$ for finite temperatures is shown. Black dots indicate the poles of the integrand.*
The right figure is a plot of $|1/(e^z+1)|$ illustrating how the Fermi-Dirac distribution function behaves at the point where $\mathcal{A}$ crosses the real line. If R is large, $\mathcal{A}$ looks like a straight line, going through this region. If we furthermore require that R is an integer multiple of 2π, the Fermi-Dirac distribution function will behave exactly like it does on the real axis.

The poles: The integrand has two poles on the real axis at a and b that deserves special attention, as they make the integral undefined. We decide to consider only the Cauchy principal value of the integral; i.e. we exclude an equally-sized small region from the domain of integration on either side of each pole.

In the closing paragraph of this section, we discuss a different method for assigning a definite value to the integral, involving adding a small imaginary value $i\eta$ to each of the guilty denominators. In section 6, the physical justification and relative merits of each of the methods are discussed.

In addition to the poles at a and b, the Fermi-Dirac distribution functions also have a series of poles. These are distributed along the imaginary axis whenever e^z equals -1, occuring at

$$z = 2\pi ni + \pi i \quad \text{for all} \quad n \in \mathbb{Z}. \tag{33}$$

The contour: We construct the contour as follows (se figure 3): The contour coincides with the real line from $-R$ to R, except from a small region around each pole. This part we call $\mathcal{L}$. The regions excluded from $\mathcal{L}$ are all z-values satisfying

$$|z-a| < \varepsilon \quad \text{or} \quad |z-b| < \varepsilon, \tag{34}$$

for some small value ϵ. The holes in $\mathcal{L}$ are connected by two pieces — named $\mathcal{C}_a$ and $\mathcal{C}_b$ — going *above* the poles. The exact shapes of $\mathcal{C}_a$ and $\mathcal{C}_b$ are irrelevant, as we are going to find their contribution through the fractional residue theorem, not direct integration.

Next, the contour arcs through the complex plane, closing the contour. The arc ($\mathcal{A}$) is parametrized by the function

$$z = e^{i\theta}R, \tag{35}$$

with θ running from 0 to π. The imaginary axis is thus crossed at the point iR. We let

$$R = 2\pi N \quad \text{with } N \in \mathbb{N} \text{ and } N \gg 1, \tag{36}$$

such that the step of the Fermi-Dirac distribution function is crossed in an approximately straight line, at one of its periodic repeats (i.e. it will behave as it does on the real axis, see figure 3).

The calculation: We call the integrand of (32) $f(z)$, i.e.

$$f(z) = \frac{1}{e^z + 1}\,\frac{1}{z-a} + \frac{1}{e^{-z}+1}\,\frac{1}{z-b}, \tag{37}$$

and let βD equal R. The Cauchy principal value of the integral in (32) can now be written as

$$\begin{aligned} P.V.\int_{-\beta D}^{\beta D} f(z)dz &= \int_{\mathcal{L}} f(z) \\ &= -\left(\int_{\mathcal{A}} + \int_{\mathcal{C}_a} + \int_{\mathcal{C}_b}\right) f(z) + 2\pi i \sum_n \text{Res}[f(z), z_n] \end{aligned} \tag{38}$$

using the residue theorem[10], where the sum runs over all poles of $f(z)$ inside the contour.

In the $\mathcal{A}$-integral we have

$$dz = ie^{i\theta}Rd\theta, \tag{39}$$

such that

$$\int_{\mathcal{A}} f(z) = i\int_0^{\pi}\left(\frac{1}{e^{e^{i\theta}R}+1}\,\frac{e^{i\theta}R}{e^{i\theta}R-a} + \frac{1}{e^{-e^{i\theta}R}+1}\,\frac{e^{i\theta}R}{e^{i\theta}R-b}\right)d\theta. \tag{40}$$

Since R is large, the Fermi-Dirac distributions become step functions and the ratios become 1, and we have

$$\int_{\mathcal{A}} f(z) = i\int_{\pi/2}^{\pi} d\theta + i\int_0^{\pi/2} d\theta = \pi i. \tag{41}$$

The sum in (38) runs over all the z-values in (33) with a positive imaginary part. I.e.

$$\begin{aligned} 2\pi i\sum_n \text{Res}[f(z), z_n] &= 2\pi i \sum_{n=0}^{N} \lim_{z\to z_n}\left(\frac{z-z_n}{e^z+1}\,\frac{1}{z-a} + \frac{z-z_n}{e^{-z}+1}\,\frac{1}{z-b}\right) \\ &= 2\pi i\sum_{n=0}^{N}\left(\frac{1}{z_n-a}\lim_{z\to z_n}\frac{z-z_n}{e^z+1} + \frac{1}{z_n-b}\lim_{z\to z_n}\frac{z-z_n}{e^{-z}+1}\right) \end{aligned} \tag{42}$$

where $z_n = (2n+1)\pi i$. By l'Hôpital's rule we have

$$\lim_{z\to z_n}\frac{z-z_n}{e^z+1} = \lim_{z\to z_n}\frac{1}{e^z} = -1, \tag{43}$$

and by similar argument

$$\lim_{z\to z_n} \frac{z-z_n}{e^{-z}+1} = 1. \tag{44}$$

We now have

$$2\pi i \sum_n \text{Res}[f(z), z_n] = -2\pi i \sum_{n=0}^{N} \left(\frac{1}{(2n+1)\pi i - a} - \frac{1}{(2n+1)\pi i - b} \right), \tag{45}$$

or by rearrangement

$$2\pi i \sum_n \text{Res}[f(z), z_n] = -\sum_{n=0}^{N} \left(\frac{1}{n+a'} - \frac{1}{n+b'} \right), \tag{46}$$

where

$$a' = \frac{1}{2} + \frac{ia}{2\pi} \quad \text{and} \quad b' = \frac{1}{2} + \frac{ib}{2\pi}. \tag{47}$$

This series is convergent; indeed for $N \to \infty$

$$\sum_{n=0}^{N} \left(\frac{1}{n+a'} - \frac{1}{n+b'} \right) = \psi(b') - \psi(a'), \tag{48}$$

where $\psi(z)$ is the digamma function.[11]

As noted above, the value of the integrals

$$\int_{\mathcal{C}_a} f(z) \quad \text{and} \quad \int_{\mathcal{C}_b} f(z) \tag{49}$$

are found using the fractional residue theorem. We have

$$\lim_{\epsilon\to 0} \int_{\mathcal{C}_a} f(z) = \phi i \, \text{Res}[f(z), a] \tag{50}$$

and similarly for b, where ϕ is the signed angle by which the contour circles the pole (e.g. $\phi = 2\pi$ would represent one entire counterclockwise circulation).[10] In our case $\phi = -\pi$ for both $\mathcal{C}_a$ and $\mathcal{C}_b$, thus

$$\begin{aligned} \lim_{\epsilon\to 0} \int_{\mathcal{C}_a} f(z) &= -\pi i \lim_{z\to a} \left(\frac{1}{e^z+1} \frac{z-a}{z-a} + \frac{1}{e^{-z}+1} \frac{z-a}{z-b} \right) \\ &= -\pi \frac{1}{e^a+1} i \end{aligned} \tag{51}$$

and

$$\lim_{\epsilon\to 0} \int_{\mathcal{C}_b} f(z) = -\pi \frac{1}{e^{-b}+1} i. \tag{52}$$

All the terms in (38) have now been uncovered. The $\mathcal{L}$-integral can be expressed as

$$\int_{\mathcal{L}} f(z) = -\left(\pi i - \pi \frac{1}{e^a+1} i - \pi \frac{1}{e^{-b}+1} i + \psi(b') - \psi(a') \right), \tag{53}$$

which looks like it might have an imaginary part, but since $f(z)$ is real everywhere on $\mathcal{L}$, this cannot be. Evidently

$$\mathrm{Im}\left(\psi(b') - \psi(a')\right) = \pi\left(\frac{1}{e^{a}+1} + \frac{1}{e^{-b}+1} - 1\right), \tag{54}$$

with a' and b' as in (47). This can be affirmed by plotting the function.

The difference between the corrections to the energies of the quantum-dot-states at finite temperatures can now be written out in full. We call this $\Delta E^{(2)}_{P.V.}$ signifying that the integral in (31) was made definite by choosing to interpret it as a Cauchy principal value integral. We have

$$\Delta E^{(2)}_{P.V.} = \frac{\Delta\Gamma}{\pi}\,\mathrm{Re}\left(\psi\left(\frac{1}{2} + \frac{i\beta\xi^{d}}{2\pi}\right) - \psi\left(\frac{1}{2} + \frac{i\beta(\xi^{d}+U)}{2\pi}\right)\right), \tag{55}$$

which is given in [6] as well.

2nd method — moving the poles: An alternative method for making the integral in (32) defined, is by moving each of the poles slightly below the real axis. This corresponds to adding $i\eta$ to each of the denominators in (32), where η is some infinitesimal number.

It would no longer be necessary for $\mathcal{L}$ to leave the real axis, so $\mathcal{C}_a$ and $\mathcal{C}_b$ could be dropped. The rest of the calculation stays the same, as $\mathcal{A}$ is unchanged and the same number of poles are enclosed. The difference in the corrections to the energy — which we shall call $\Delta E^{(2)}_{\eta}$ in this case — becomes

$$\Delta E^{(2)}_{\eta} = \Delta E^{(2)}_{P.V.} + i\Delta\Gamma\left(\frac{1}{e^{\beta(\xi^{d}+U)}+1} + \frac{1}{e^{-\beta\xi^{d}}+1}\right). \tag{56}$$

6 Self Energy

All the terms in the complete Hamiltonian of the modelled system are quadratic in fermionic creation and annihilation operators. The sole exception being the term

$$U d^{\dagger}_{\uparrow} d_{\uparrow} d^{\dagger}_{\downarrow} d_{\downarrow} \tag{57}$$

of $H_{\ell d}$, which is quartic. The presence of this term makes it in general impossible to find exact Green's functions for the system.[7]

Setting $U = 0$, equivalent to turning of all interactions between electrons in the system, leads to a model for which the associated Green's functions in principle can be found explicitly, and for which the concept of self energy naturally emerges. The system reduces to a model treated in [7] under the heading "Single level coupled to continuum". The arguments are presented in the following section.

6.1 Quantum dot self energy

The model described in section 3.1 is altered by setting U to zero as described above. This makes the $\uparrow$-state and the $\downarrow$-state of the quantum dot independent

of each other, and makes the calculations applied to this two-level system almost identical to the one-level system described in [7]. This subsection follows the derivation in [7] closely.

The diagonal retarded Green's function for propagation in quantum dot states is defined as

$$G^R_{dd}(\sigma,t) = -i\theta(t)\left\langle\left\{d_\sigma(t), d^\dagger_\sigma\right\}\right\rangle, \tag{58}$$

where $\langle\cdots\rangle$ represents thermal averaging over all states, $\theta(t)$ is the Heaviside step function and $\{\,\cdot\,,\,\cdot\,\}$ represents the anti-commutator. This function is found using the equation of motion technique.

The Green's function is differentiated with respect to time to yield

$$\tfrac{d}{dt}G^R_{dd}(\sigma,t) = -i\delta(t) - i\theta(t)\left\langle\left\{\tfrac{d}{dt}\left(d_\sigma(t)\right), d^\dagger_\sigma\right\}\right\rangle, \tag{59}$$

where we used that $d_\sigma(t) = d_\sigma$ for $t = 0$, and that anti-commuting same state fermionic creation and annihilation operators yields one. The time dependance of $d_\sigma(t)$ is given in the Heisenberg picture as

$$\tfrac{d}{dt}\left(d_\sigma(t)\right) = i[H, d_\sigma](t), \tag{60}$$

where

$$\left[H, d_\sigma\right] = -\xi^d_\sigma d_\sigma - \sum_{\boldsymbol{k}} T_{\boldsymbol{k}\sigma} c_{\boldsymbol{k}\sigma}. \tag{61}$$

Here we used that

$$\left[d^\dagger_{\sigma'} c_{\boldsymbol{k}\sigma'}, d_\sigma\right] = d^\dagger_{\sigma'}\left\{c_{\boldsymbol{k}\sigma'}, d_\sigma\right\} - \left\{d^\dagger_{\sigma'}, d_\sigma\right\} c_{\boldsymbol{k}\sigma'} = -\delta_{\sigma\sigma'} c_{\boldsymbol{k}\sigma}. \tag{62}$$

Multiplying both sides of (59) by i yields

$$i\tfrac{d}{dt}G^R_{dd}(\sigma,t) = \delta(t) + \xi^d_\sigma G^R_{dd}(\sigma,t) + \sum_{\boldsymbol{k}} T_{\boldsymbol{k}\sigma} G^R_{\ell d}(\boldsymbol{k}\sigma,t), \tag{63}$$

where

$$G^R_{\ell d}(\boldsymbol{k}\sigma,t) \equiv -i\theta(t)\left\langle\left\{c_{\boldsymbol{k}\sigma}(t), d^\dagger_\sigma\right\}\right\rangle. \tag{64}$$

Repeating the process for $G^R_{\ell d}(\boldsymbol{k}\sigma,t)$ produces

$$i\tfrac{d}{dt}G^R_{\ell d}(\boldsymbol{k}\sigma,t) = \xi^\ell_{\boldsymbol{k}\sigma} G^R_{\ell d}(\boldsymbol{k}\sigma,t) + T^*_{\boldsymbol{k}\sigma} G^R_{dd}(\sigma,t). \tag{65}$$

Here we used that

$$\left[H, c_{\boldsymbol{k}\sigma}\right] = -\xi^\ell_{\boldsymbol{k}\sigma} c_{\boldsymbol{k}\sigma} - T^*_{\boldsymbol{k}\sigma} d_\sigma. \tag{66}$$

To turn these expressions into an algebraic equation, we perform a Fourier transform. However, a slightly modified version of the standard time to frequency Fourier Transform is used; this is defined by

$$f(\omega) = \int_{-\infty}^{\infty} dt\, f(t) e^{i(\omega+i\eta)t}, \tag{67}$$

where η is an infinitesimal positive value. The introduction of $i\eta$ into the normal definition of the Fourier transform is physically motivated. Since ηt vanishes for all reasonable values of t, the Fourier transform as defined above is identical to the standard Fourier transform, as long as a finite t' exists, such that

$$f(t) = 0 \quad \text{for all} \quad t > t'. \tag{68}$$

The Green's functions above are related to the correlation between adding an electron to the quantum dot σ-state or the lead $\boldsymbol{k}\sigma$-state at time 0, and later finding an electron in the σ-state of the quantum dot at time t. Thus any kind of relaxation will satisfy the above requirement.[7, 12]

The Fourier transform of the two expressions above are

$$\begin{aligned}(\omega + i\eta)G^R_{dd}(\sigma,\omega) &= 1 + \xi^d_\sigma G^R_{dd}(\sigma,\omega) + \sum_{\boldsymbol{k}} T_{\boldsymbol{k}\sigma} G^R_{\ell d}(\boldsymbol{k}\sigma,\omega) \\ \text{and} \quad (\omega + i\eta)G^R_{\ell d}(\boldsymbol{k}\sigma,\omega) &= \xi^\ell_{\boldsymbol{k}\sigma} G^R_{\ell d}(\boldsymbol{k}\sigma,\omega) + T^*_{\boldsymbol{k}\sigma} G^R_{dd}(\sigma,\omega).\end{aligned} \tag{69}$$

Here we used that

$$\int_{-\infty}^{\infty} dt \, \left(\tfrac{d}{dt} f(t)\right) e^{i(\omega+i\eta)t} = -i(\omega + i\eta) f(\omega) \tag{70}$$

(through integration by parts) and

$$\int_{-\infty}^{\infty} dt \, \delta(t) e^{i(\omega+i\eta)t} = 1. \tag{71}$$

The equations in (69) are algebraic equations with the solution

$$G^R_{dd}(\sigma,\omega) = \frac{1}{\omega + i\eta - \xi^d_\sigma - \Sigma^R_d(\sigma,\omega)} \tag{72}$$

where

$$\Sigma^R_d(\sigma,\omega) \equiv \sum_{\boldsymbol{k}} \frac{|T_{\boldsymbol{k}\sigma}|^2}{\omega + i\eta - \xi^\ell_{\boldsymbol{k}\sigma}} \tag{73}$$

is the self energy of the quantum dot states. This should be compared with the term

$$\sum_{\boldsymbol{k}} \frac{|T_{\boldsymbol{k}\sigma}|^2}{-\xi^\ell_{\boldsymbol{k}\sigma} + \xi^d_\sigma} \tag{74}$$

of (17), which contributes to the second order correction to the energy of the quantum dot σ-state. Inserting ξ^d_σ — the base energy of the state — makes the comparison more obvious. In the following sections, we extend this line of calculations to recover self-energies corresponding to the remaining terms in (17), and explain the similarity.

6.2 Self energy of lead states

We now turn to the lead states. We define the diagonal Green's function for propagation in the lead as

$$G^R_{\ell\ell}(\boldsymbol{k}\sigma, t) \equiv -i\theta(t) \left\langle \left\{ c_{\boldsymbol{k}\sigma}(t), c^\dagger_{\boldsymbol{k}\sigma} \right\} \right\rangle . \tag{75}$$

Differentiation yields

$$i\tfrac{d}{dt} G^R_{\ell\ell}(\boldsymbol{k}\sigma, t) = \delta(t) + \xi^\ell_{\boldsymbol{k}\sigma} G^R_{\ell\ell}(\boldsymbol{k}\sigma, t) + T^*_{\boldsymbol{k}\sigma} G^R_{d\ell}(\boldsymbol{k}\sigma, t) \tag{76}$$

where we reused (66). $G^R_{d\ell}(\boldsymbol{k}\sigma, t)$ is defined by

$$G^R_{d\ell}(\boldsymbol{k}\sigma, t) \equiv -i\theta(t) \left\langle \left\{ d_\sigma(t), c^\dagger_{\boldsymbol{k}\sigma} \right\} \right\rangle . \tag{77}$$

Differentiating this function will give rise to non-diagonal Green's function between lead states. These are not zero, as they could be connected through further coupling to the quantum dot, and back. However, here we choose to neglect these Green's functions, as their inclusion in the $G^R_{\ell\ell}$-function would make $H_{\ell d}$ enter at fourth order, whereas the energy corrections in section 5 — to which we seek to compare these self-energies — only include second order processes. With this in mind, we obtain

$$i\frac{d}{dt} G^R_{d\ell}(\boldsymbol{k}\sigma, t) = \xi^d_\sigma G^R_{d\ell}(\boldsymbol{k}\sigma, t) + T_{\boldsymbol{k}\sigma} G^R_{\ell\ell}(\boldsymbol{k}\sigma, t), \tag{78}$$

using

$$\left[H, d_\sigma \right] = -\xi^d_\sigma d_\sigma - \sum_{\boldsymbol{k}'} T_{\boldsymbol{k}'\sigma} c_{\boldsymbol{k}'\sigma} \tag{79}$$

but neglecting all non-diagonal entries in the sum (entries where $\boldsymbol{k}' \neq \boldsymbol{k}$).

Performing the Fourier transforms as before and solving the algebraic equations which emerges, leads to

$$G^R_{\ell\ell}(\boldsymbol{k}\sigma, \omega) = \frac{1}{\omega + i\eta - \xi^\ell_{\boldsymbol{k}\sigma} - \Sigma^R_\ell(\boldsymbol{k}\sigma, \omega)} \tag{80}$$

where

$$\Sigma^R_\ell(\boldsymbol{k}\sigma, \omega) \equiv \frac{|T_{\boldsymbol{k}\sigma}|^2}{\omega + i\eta - \xi^d_\sigma}. \tag{81}$$

This gives the self energy of a single lead state. To compare this to (17), we need to sum over the occupied states of the lead, when in thermal equilibrium. We obtain

$$\sum_{\boldsymbol{k}\sigma} \frac{|T_{\boldsymbol{k}\sigma}|^2 \, n_F(\xi_{\boldsymbol{k}\sigma})}{\xi_{\boldsymbol{k}\sigma} + i\eta - \xi^d_\sigma} \tag{82}$$

which corresponds to the last two terms of (17), provided that U is zero. If U is not zero, we cannot directly associate the second order correction found through standard perturbation theory with any self energy, however the generalization is obvious.

If we permit ourselves to view (17) as an expression involving self-energies, we can reintroduce the term $i\eta$, justifying the two mathematical methods employed in 5.1.2. Moving the poles gives the self energy, and taking the Cauchy principal value simply isolates the real part.

6.3 The imaginary part of the self energy

In general the imaginary part of a self energy is proportional to reciprocal of the lifetime of particles in the state.[7, 12]

This also holds for the difference in the energy correction between the quantum dot states found in (5.1.2). I.e. the difference in transition rates found in the following section, reflects the difference in lifetime found from the imaginary part of the expression obtained in (5.1.2) for $\Delta E_\eta^{(2)}$, up to second order in $T_{k\sigma}$.

7 Transition Rates

The transition rates going from a singly occupied dot with a definite spin, to one of the other available states, can be calculated to first order in $H_{\ell d}$ using Fermi's golden rule, and to higher orders using a generalized version.

The generalized Fermi's golden rule[7] can be written as

$$R_{fi} = 2\pi \left|\langle f| \, T \, |i\rangle\right|^2 \delta(E_f - E_i) \tag{83}$$

where

$$T = V + V\frac{1}{E_i - H_0 + i\eta}T. \tag{84}$$

Here R_{fi} is the transition rate from the initial state $|i\rangle$ to the final state $|f\rangle$ (normally denoted Γ_{fi}), H_0 is the unperturbed Hamiltonian which E_i and E_f are given in relation to and V is the perturbation.

In this section we pursue this formula up to second order for $|i\rangle$ being a state of the form $|\sigma\rangle_d \, |a\rangle_\ell$ with thermal averaging over $|a\rangle_\ell$ states. For each order, we sum over all possible final states.

7.1 First order

To first order in $H_{\ell d}$, the transition rate from state $|i\rangle$ to $|f\rangle$ reads

$$R_{fi}^{(1)} = 2\pi \left| \langle f| \left(\sum_{k\sigma} T_{k\sigma} d_\sigma^\dagger c_{k\sigma} + \sum_{k\sigma} T_{k\sigma}^* c_{k\sigma}^\dagger d_\sigma \right) |i\rangle \right|^2 \delta(E_f - E_i). \tag{85}$$

If $|i\rangle$ is of the form $|a\rangle_d \, |\sigma\rangle_\ell$, then only final states that can be written as

$$c_{k\sigma}^\dagger \, |a\rangle_d \, |0\rangle_\ell \quad \text{or} \quad c_{k\bar{\sigma}} \, |a\rangle_d \, |\uparrow\downarrow\rangle_\ell \tag{86}$$

will yield non-zero inner products. For each case we have

$$R_{k\,0,\,a\sigma}^{(1)} = 2\pi \left|T_{k\sigma}\right|^2 \left| \langle a|_\ell \left(1 - c_{k\sigma}^\dagger c_{k\sigma}\right) |a\rangle_\ell \right|^2 \delta(\xi_{k\sigma}^\ell - \xi_\sigma^d) \tag{87}$$

$$R_{k\uparrow\downarrow,\,a\sigma}^{(1)} = 2\pi \left|T_{k\bar{\sigma}}\right|^2 \left| \langle a|_\ell \, c_{k\bar{\sigma}}^\dagger c_{k\bar{\sigma}} \, |a\rangle_\ell \right|^2 \delta(\xi_{\bar{\sigma}}^d + U - \xi_{k\bar{\sigma}}^\ell). \tag{88}$$

Again, if $|a\rangle_\ell$ is a Fock state, $|\cdots|^2$ acts as the identity function. Therefore, taking the thermal average — similar to the calculation in section 5 — yields

$$R^{(1)}_{\boldsymbol{k}\,0,\sigma} = 2\pi\,|T_{\boldsymbol{k}\sigma}|^2\left(1 - n_F(\xi^\ell_{\boldsymbol{k}\sigma})\right)\delta(\xi^\ell_{\boldsymbol{k}\sigma} - \xi^d_\sigma) \tag{89}$$

$$R^{(1)}_{\boldsymbol{k}\uparrow\downarrow,\sigma} = 2\pi\,|T_{\boldsymbol{k}\bar{\sigma}}|^2\, n_F(\xi^\ell_{\boldsymbol{k}\bar{\sigma}})\delta(\xi^d_{\bar{\sigma}} + U - \xi^\ell_{\boldsymbol{k}\bar{\sigma}}). \tag{90}$$

We now intend to sum over the possible final states. Assuming the same restrictions on the relation between $\boldsymbol{k}$, $\xi^\ell_{\boldsymbol{k}\sigma}$ and $T_{\boldsymbol{k}\sigma}$ as was used in section 5.1, the sum can be converted to an integral. I.e.

$$R^{(1)}_{0,\sigma} = \int_\xi \mathcal{D}_\sigma(\xi)2\pi\,|T_\sigma(\xi)|^2\,(1 - n_F(\xi))\,\delta(\xi - \xi^d_\sigma)d\xi \tag{91}$$

$$R^{(1)}_{\uparrow\downarrow,\sigma} = \int_\xi \mathcal{D}_{\bar{\sigma}}(\xi)2\pi\,|T_{\bar{\sigma}}(\xi)|^2\, n_F(\xi)\delta(\xi^d_{\bar{\sigma}} + U - \xi)d\xi. \tag{92}$$

Performing the integrals, the transition rates can be written as

$$R^{(1)}_{0,\sigma} = 2\Gamma_\sigma(\xi^d_\sigma)\left(1 - n_F(\xi^d_\sigma)\right) \tag{93}$$

$$R^{(1)}_{\uparrow\downarrow,\sigma} = 2\Gamma_{\bar{\sigma}}(\xi^d_{\bar{\sigma}} + U)n_F(\xi^d_{\bar{\sigma}} + U) \tag{94}$$

using the coupling defined earlier.

As discussed in section 6.3, this rate reflects the imaginary part of $\Delta E^{(2)}_\eta$. To se this, we calculate the difference in rate between spin up and spin down using the same approximations as in section 5.1.2. We have

$$\Delta R^{(1)} = 2\Delta\Gamma\left(\frac{1}{e^{\beta(\xi^d + U)} + 1} + \frac{1}{e^{-\beta\xi^d} + 1}\right). \tag{95}$$

This is twice the magnitude of the imaginary part of $\Delta E^{(2)}_\eta$, however this rate refers to the rate of change of probability, while the imaginary part of $\Delta E^{(2)}_\eta$ gives the reciprocal lifetime of probability amplitude.[7, 12] In other words

$$|e^{-(\tau^{-1})t}|^2 = e^{-2(\tau^{-1})t}, \tag{96}$$

explaining the factor of two.

7.2 Second order

The second-order part of the transition rate, going from the Fock-state $|\sigma\rangle_d\,|a\rangle_\ell$ to $|f\rangle$ can be expressed as

$$R^{(2)}_{f,a\sigma} = 2\pi\left|\langle f|\,H_{\ell d}\frac{1}{E_i - H_0 + i\eta}H_{\ell d}\,|\sigma\rangle_d\,|a\rangle_\ell\right|^2\delta(E_f - E_{a\sigma}). \tag{97}$$

If the sums in each of the two $H_{\ell d}$-operators are expanded, different combinations of creation and annihilation operators appear. Considering only the quantum dot operators, sixteen combinations are possible. Of these sixteen, four combinations involves putting two extra electrons on the quantum dot,

which is already occupied by one electron. These combinations yield zero. Similarly, four combinations involves removing two electrons from the dot. Of the remaining eight, two involves emptying the already empty $\overline{\sigma}$-state, and two involves filling the already full σ-state.

The remaining four combinations, leads to only three different classes of final states, reached by four different virtual processes:

1. *Combination:* $d^\dagger_\sigma c_{\boldsymbol{k}'\sigma} c^\dagger_{\boldsymbol{k}\sigma} d_\sigma$.
   Virtual process: An electron is moved from the σ-state of the quantum dot to a $\boldsymbol{k}\sigma$-state on the lead, then an electron is moved from a $\boldsymbol{k}'\sigma$-state on the lead to the σ-state of the dot.
   Final state: $c_{\boldsymbol{k}'\sigma} c^\dagger_{\boldsymbol{k}\sigma} \left|\sigma\right\rangle_d \left|a\right\rangle_\ell$.
   Note that energy conservations requires degeneracy between the $\boldsymbol{k}\sigma$-lead-state and the $\boldsymbol{k}'\sigma$-lead-state.

2. *Combination:* $d^\dagger_{\overline{\sigma}} c_{\boldsymbol{k}'\overline{\sigma}} c^\dagger_{\boldsymbol{k}\sigma} d_\sigma$.
   Virtual process: Intermittent empty quantum dot.
   Final state: $c_{\boldsymbol{k}'\overline{\sigma}} c^\dagger_{\boldsymbol{k}\sigma} \left|\overline{\sigma}\right\rangle_d \left|a\right\rangle_\ell$.

3. *Combination:* $c^\dagger_{\boldsymbol{k}'\sigma} d_\sigma d^\dagger_{\overline{\sigma}} c_{\boldsymbol{k}\overline{\sigma}}$.
   Virtual process: Intermittent doubly occupied quantum dot.
   Final state: $c^\dagger_{\boldsymbol{k}'\sigma} c_{\boldsymbol{k}\overline{\sigma}} \left|\overline{\sigma}\right\rangle_d \left|a\right\rangle_\ell$.

4. *Combination:* $c^\dagger_{\boldsymbol{k}'\overline{\sigma}} d_{\overline{\sigma}} d^\dagger_{\overline{\sigma}} c_{\boldsymbol{k}\overline{\sigma}}$.
   Virtual process: Intermittent doubly occupied quantum dot.
   Final state: $c^\dagger_{\boldsymbol{k}'\overline{\sigma}} c_{\boldsymbol{k}\overline{\sigma}} \left|\sigma\right\rangle_d \left|a\right\rangle_\ell$.
   Again, this process requires degeneracy.

Here we look only at combinations number 2 and 3, which flip the spin of the quantum dot. For these combinations, the classes of final states overlap completely; interchanging the names of the dummy variables $\boldsymbol{k}$ and $\boldsymbol{k}'$ reveals that the wave vectors can be chosen such that the states are identical (except for an opposite phase).

We denote the second-order part of the transfer rate to the state $c^\dagger_{\boldsymbol{k}\sigma} c_{\boldsymbol{k}'\overline{\sigma}} \left|\overline{\sigma}\right\rangle_d \left|a\right\rangle_\ell$ from $\left|\sigma\right\rangle_d \left|a\right\rangle_\ell$ as $R^{(2)}_{\boldsymbol{k}'\boldsymbol{k}a\sigma}$. We have

$$
\begin{aligned}
R^{(2)}_{\boldsymbol{k}'\boldsymbol{k}a\sigma} &= 2\pi \left| \left\langle a\right|_\ell \left\langle \overline{\sigma}\right|_d c^\dagger_{\boldsymbol{k}'\overline{\sigma}} c_{\boldsymbol{k}\sigma} \left(\cdots\right) \left|\sigma\right\rangle_d \left|a\right\rangle_\ell \right|^2 \delta(E_f - E_{a\sigma}) \\
\left(\cdots\right) &= \left(\frac{T_{\boldsymbol{k}'\overline{\sigma}} d^\dagger_{\overline{\sigma}} c_{\boldsymbol{k}'\overline{\sigma}} T^*_{\boldsymbol{k}\sigma} c^\dagger_{\boldsymbol{k}\sigma} d_\sigma}{\xi^d_\sigma - \xi^\ell_{\boldsymbol{k}\sigma} + i\eta} + \frac{T^*_{\boldsymbol{k}\sigma} c^\dagger_{\boldsymbol{k}\sigma} d_\sigma T_{\boldsymbol{k}'\overline{\sigma}} d^\dagger_{\overline{\sigma}} c_{\boldsymbol{k}'\overline{\sigma}}}{\xi^\ell_{\boldsymbol{k}'\overline{\sigma}} - \xi^d_{\overline{\sigma}} - U + i\eta} \right).
\end{aligned}
\tag{98}
$$

To make the two sets of operators look alike involves the movement of two fermionic operators past two other fermionic operators operating on different states. This requires four changes of sign, canceling out one another. The quantum dot operators can be moved to either side making the quantum dot part

of the inner product yield one. Factoring out as much as possible, we have

$$\begin{aligned} R^{(2)}_{\boldsymbol{k}'\boldsymbol{k}a\sigma} &= 2\pi \left|T_{\boldsymbol{k}\sigma}\right|^2 \left|T_{\boldsymbol{k}'\overline{\sigma}}\right|^2 |IP|^2 \, |A|^2 \, \delta(\xi^{\ell}_{\boldsymbol{k}\sigma} + \xi^{d}_{\overline{\sigma}} - \xi^{\ell}_{\boldsymbol{k}'\overline{\sigma}} - \xi^{d}_{\sigma}) \\ IP &= \langle a|_{\ell} \, c^{\dagger}_{\boldsymbol{k}'\overline{\sigma}} c_{\boldsymbol{k}'\overline{\sigma}} c_{\boldsymbol{k}\sigma} c^{\dagger}_{\boldsymbol{k}\sigma} \, |a\rangle_{\ell} = \langle a|_{\ell} \, c^{\dagger}_{\boldsymbol{k}'\overline{\sigma}} c_{\boldsymbol{k}'\overline{\sigma}} (1 - c^{\dagger}_{\boldsymbol{k}\sigma} c_{\boldsymbol{k}\sigma}) \, |a\rangle_{\ell} \\ A &= \frac{1}{\xi^{d}_{\sigma} - \xi^{\ell}_{\boldsymbol{k}\sigma} + i\eta} + \frac{1}{\xi^{\ell}_{\boldsymbol{k}'\overline{\sigma}} - \xi^{d}_{\overline{\sigma}} - U + i\eta}. \end{aligned} \tag{99}$$

Again, the inner product yields one or zero, hence $|IP|^2$ equals IP. We perform the thermal average over a states, yielding

$$R^{(2)}_{\boldsymbol{k}'\boldsymbol{k}\sigma} = 2\pi \left|T_{\boldsymbol{k}\sigma}\right|^2 \left|T_{\boldsymbol{k}'\overline{\sigma}}\right|^2 n_F(\xi^{\ell}_{\boldsymbol{k}'\overline{\sigma}}) \left(1 - n_F(\xi^{\ell}_{\boldsymbol{k}\sigma})\right) |A|^2 \, \delta(\cdots). \tag{100}$$

We now sum over different possible final states. As before, we change the sum to integrals using

$$\sum_{\boldsymbol{k}} |T_{\boldsymbol{k}\sigma}|^2 f(\xi^{\ell}_{\boldsymbol{k}\sigma}) = \frac{1}{\pi} \int_{\xi} \Gamma_{\sigma}(\xi) f(\xi) d\xi, \tag{101}$$

and obtain

$$\begin{aligned} R^{(2)}_{\sigma} = \frac{2}{\pi} \int d\xi \int d\xi' \, \Gamma_{\sigma}(\xi) \Gamma_{\overline{\sigma}}(\xi') n_F(\xi') \, (1 - n_F(\xi)) \times \\ \times \left| \frac{1}{\xi^{d}_{\sigma} - \xi + i\eta} + \frac{1}{\xi' - \xi^{d}_{\overline{\sigma}} - U + i\eta} \right|^2 \delta(\xi + \xi^{d}_{\overline{\sigma}} - \xi' - \xi^{d}_{\sigma}). \end{aligned} \tag{102}$$

The inner integral is solved by utilizing the Dirac-delta function, the argument to which is zero whenever

$$\xi' = \xi + \xi^{d}_{\overline{\sigma}} - \xi^{d}_{\sigma}. \tag{103}$$

Adopting this as a definition of ξ', we can write

$$R^{(2)}_{\sigma} = \frac{2}{\pi} \int d\xi \, \Gamma_{\sigma}(\xi) \Gamma_{\overline{\sigma}}(\xi') n_F(\xi') \, (1 - n_F(\xi)) \, |\cdots|^2 , \tag{104}$$

where A has been omitted. The remainder of this section deals with the application of this general formula, within the flat band approximation.

7.2.1 Flat band at low temperatures

The essence of the flat band approximation lies in (21), restated here for convenience:

$$\Gamma_{\sigma}(\xi) = \begin{cases} \Gamma_{\sigma} & \text{if } |\xi| < D \\ 0 & \text{otherwise.} \end{cases} \tag{105}$$

With this approximation (104) becomes

$$R^{(2)}_{\sigma} = \frac{2\Gamma_{\sigma}\Gamma_{\overline{\sigma}}}{\pi} \int_{-D}^{D} d\xi \, n_F(\xi') \, (1 - n_F(\xi)) \, |\cdots|^2 . \tag{106}$$

Furthermore, we assume as before that the external magnetic field is well aligned, to make the singly occupied quantum dot states nearly degenerate. In this case we have

$$\xi' \approx \xi, \tag{107}$$

and (106) becomes

$$R_\sigma^{(2)} = \frac{2\Gamma_\sigma\Gamma_{\overline{\sigma}}}{\pi}\int_{-D}^{D} d\xi\, \frac{1}{e^{\beta\xi}+1}\frac{1}{e^{-\beta\xi}+1}\times \\ \times\left|\frac{1}{\xi^d-\xi+i\eta}+\frac{1}{\xi-\xi^d-U+i\eta}\right|^2. \tag{108}$$

At 0 °K, the Fermi-Dirac distribution functions conspire to make the integrand zero for all values of ξ. For any finite temperature however, the behaviour around the poles makes the integral tend to infinity as $\eta \to 0$. This is different from the behaviour of the integral studied in section 5.1.2, and no mathematical tricks will come up with a reasonable solution to this integral.

A possible resolution lies in a less abstract interpretation of the T-matrix given in (84). Considering the fractions in (84) as propagators, interspersed by scattering events, opens up for the possibility of a self energy. We imagine that this self energy has an imaginary part with a magnitude of Λ, this would correspond to a lifetime of approximately Λ^{-1}.

With the imaginary part $i\Lambda$ added to each of the denominators, we obtain an expression which does not diverge. Since Λ is much larger than η, η can be dropped. The integrand — which we shall call $f(\xi)$ — now reads

$$\frac{1}{e^{\beta\xi}+1}\frac{1}{e^{-\beta\xi}+1}\left|\frac{1}{\xi^d-\xi+i\Lambda}+\frac{1}{\xi-\xi^d-U+i\Lambda}\right|^2. \tag{109}$$

If

$$\beta\xi^d \ll 0 \quad \text{and} \quad 0 \ll \beta\left(\xi^d+U\right) \tag{110}$$

such that both the singly occupied and the doubly occupied energy-levels of the dot are far away from the Fermi-level compared to k_BT. The above expression is dominated by three contributions, well separated along the ξ-axis.

First, at the pole near ξ^d+U, we have for small Λ.

$$f(\xi^d+U+\delta) = \frac{1}{e^{\beta(\xi^d+U)}+1}\frac{1}{e^{-\beta(\xi^d+U)}+1}\left|\frac{1}{\delta+i\Lambda}\right|^2, \tag{111}$$

which is slightly smaller than

$$\frac{1}{e^{\beta(\xi^d+U)}}\left|\frac{1}{\delta+i\Lambda}\right|^2. \tag{112}$$

Integrating this over δ yields

$$\frac{1}{e^{\beta(\xi^d+U)}}\frac{\pi}{\Lambda}. \tag{113}$$

The contribution to the integral from the other pole is similarly bounded by

$$\frac{1}{e^{-\beta\xi^d}}\frac{\pi}{\Lambda}. \tag{114}$$

The final contribution to the integral is attributed to the area near $\xi = 0$, where the integrand is not exponentially suppressed. With the approximation explained in (110), ξ vanishes compared to the quantum dot energy levels in the denominators. We have for $|\xi| \ll k_b T$

$$\begin{aligned} f(\xi) &= \frac{1}{e^{\beta\xi}+1}\frac{1}{e^{-\beta\xi}+1}\left|\frac{1}{\xi^d + i\Lambda} + \frac{1}{-\xi^d - U + i\Lambda}\right|^2 \\ &= \frac{1}{e^{\beta\xi}+1}\frac{1}{e^{-\beta\xi}+1}\frac{4\Lambda^2 + U^2}{((\xi^d)^2+\Lambda^2)\left((\xi^d+U)^2+\Lambda^2\right)}, \end{aligned} \tag{115}$$

which for small Λ becomes

$$f(\xi) = \frac{1}{e^{\beta\xi}+1}\frac{1}{e^{-\beta\xi}+1}\left(\frac{U}{\xi^d(\xi^d+U)}\right)^2. \tag{116}$$

Integrating this over ξ yields

$$\frac{1}{\beta}\left(\frac{U}{\xi^d(\xi^d+U)}\right)^2. \tag{117}$$

To summarize; within the approximation

$$(k_B T \text{ and } \Lambda) \ll \left(|\xi^d| \text{ and } |\xi^d + U|\right), \tag{118}$$

we have

$$R_\sigma^{(2)} \approx \frac{2\Gamma_\sigma\Gamma_{\overline{\sigma}}}{\pi}\left(\frac{1}{\beta}\left(\frac{U}{\xi^d(\xi^d+U)}\right)^2 + \frac{\pi}{\Lambda}\left(\frac{1}{e^{\beta(\xi^d+U)}} + \frac{1}{e^{-\beta\xi^d}}\right)\right). \tag{119}$$

We see, that for energy levels nearing the Fermi level, the spin flip rates will increase dramatically.

Assuming that ξ^d and $\xi^d + U$ are both on the order of ζ from the Fermi level, the condition

$$\Lambda \gg \frac{\beta\zeta^2}{e^{\beta\zeta}} \tag{120}$$

will validate the approximation

$$R_\sigma^{(2)} \approx \frac{2\Gamma_\sigma\Gamma_{\overline{\sigma}}}{\pi}\frac{1}{\beta}\left(\frac{U}{\xi^d(\xi^d+U)}\right)^2. \tag{121}$$

In this case $R_\sigma^{(2)}$, will be directly proportional to the temperature.

8 Conclusion

8.1 Issues

In spite of the apparent simplicity of the system investigated in this project, the theory needed to resolve even basic properties of the system turned out to be very involved. Even for the simplistic flat band model, it was necessary to perform a multitude of approximation in order to obtain any sort of information regarding the energy levels at finite temperatures.

The concept of a self energy, specifically the imaginary part of the self energy — proportional to the inverse lifetime — was central to both the energy level calculations and the calculations of transition rates.

The results of the energy level corrections in tandem with first order transition rates seemed to justify the interpretation of the energy corrections as a form of self energy. However, this connection could not be shown explicitly because of the quartic term

$$U d_\uparrow^\dagger d_\uparrow d_\downarrow^\dagger d_\downarrow \tag{122}$$

of H_d.

8.2 Results

The first order correction to the energy of the quantum dot states ($E_\sigma^{(1)}$) was found to be zero in all cases.

In the context of the flat band model, the second order correction to the energy was found to be dependent on the slightly artificial parameter D for the half-width of the band. The difference however, was found to be independent of D, and an exact solution was recovered using contour integration. This solution was later shown to have interesting analytical properties, connected to the lifetime of the quantum dot states.

The transition rates for second order processes flipping the spin of the quantum dot was approximated. This approximation was based on the introduction of an imaginary part to the quantum dot energy levels. The approximation is also limited to ranges of ξ^d and $\xi^d + U$ far away from the Fermi level compared to $k_B T$, but these are arguably the most interesting, as these ranges insure that the spin flip rate is low.

Appendix

A.1 Derivation of the Fermi-Dirac distribution

We return to the expression

$$\frac{\sum_a e^{-\beta E_a^\ell} \langle a|_\ell \, c_{\boldsymbol{k}\sigma}^\dagger c_{\boldsymbol{k}\sigma} \, |a\rangle_\ell}{\sum_a e^{-\beta E_a^\ell}} \tag{123}$$

from (17). Here the sums run over all lead Fock states. We split the sums in two, where the first part runs over all the states without an electron in the $\boldsymbol{k}\sigma$-state and the second part runs over the same states with the electron added

back in.

$$\frac{\sum_b e^{-\beta E_b^\ell} \langle b|_\ell \, c_{\boldsymbol{k}\sigma}^\dagger c_{\boldsymbol{k}\sigma} \, |b\rangle_\ell + \sum_b e^{-\beta(E_b^\ell + \xi_{\boldsymbol{k}\sigma}^\ell)} \langle b|_\ell \, c_{\boldsymbol{k}\sigma} c_{\boldsymbol{k}\sigma}^\dagger c_{\boldsymbol{k}\sigma} c_{\boldsymbol{k}\sigma}^\dagger \, |b\rangle_\ell}{\sum_b e^{-\beta E_b^\ell} + \sum_b e^{-\beta(E_b^\ell + \xi_{\boldsymbol{k}\sigma}^\ell)}}$$

$$= \frac{\sum_b e^{-\beta(E_b^\ell + \xi_{\boldsymbol{k}\sigma}^\ell)}}{\sum_b e^{-\beta E_b^\ell} + \sum_b e^{-\beta(E_b^\ell + \xi_{\boldsymbol{k}\sigma}^\ell)}} = \frac{e^{-\beta \xi_{\boldsymbol{k}\sigma}^\ell} \sum_b e^{-\beta E_b^\ell}}{\sum_b e^{-\beta E_b^\ell} + e^{-\beta \xi_{\boldsymbol{k}\sigma}^\ell} \sum_b e^{-\beta E_b^\ell}}$$

$$= \frac{e^{-\beta \xi_{\boldsymbol{k}\sigma}^\ell}}{1 + e^{-\beta \xi_{\boldsymbol{k}\sigma}^\ell}} = \frac{1}{e^{\beta \xi_{\boldsymbol{k}\sigma}^\ell} + 1} = n_F(\xi_{\boldsymbol{k}\sigma}^\ell). \tag{124}$$

References

[1] David J. Griffiths. *Introduction to Quantum Mechanics*. Pearson Prentice Hall, 2nd edition, 2007.

[2] B. Schumacher. Quantum coding. *Physical Review A*, 51(4):2738–2747, 1995.

[3] Pierre M. Petroff, Axel Lorke, and Atac Imamoglu. Epitaxially self-assembled quantum dots. *Physics Today*, 54(5):46–52, 2001.

[4] J. M. Elzerman, R. Hanson, J. S. Greidanus, L. H. Willems van Beveren, S. De Franceschi, L. M. K. Vandersypen, S. Tarucha, and L. P. Kouwenhoven. Few-electron quantum dot circuit with integrated charge read out. *Phys. Rev. B*, 67(16):161308, Apr 2003.

[5] J. R. Hauptmann, J. Paaske, and P. E. Lindelof. Electric-field-controlled spin reversal in a quantum dot with ferromagnetic contacts. *Nat Phys*, 4(5):373–376, May 2008.

[6] M. Sindel, L. Borda, J. Martinek, R. Bulla, J. Konig, G. Schon, S. Maekawa, and J. von Delft. Kondo quantum dot coupled to ferromagnetic leads: Numerical renormalization group study. *Physical Review B (Condensed Matter and Materials Physics)*, 76(4):045321–17, July 2007.

[7] Henrik Bruus and Karsten Flensberg. *Many-Body Quantum Theory in Condensed Matter Physics: An Introduction*. Oxford University Press, USA, November 2004.

[8] Charles Kittel. *Introduction to Solid State Physics*. Wiley, 8th edition, November 2004.

[9] D. C. Tsui. de haas-van alphen effect and electronic band structure of nickel. *Physical Review*, 164(2):669–683.

[10] Theodore W. Gamelin. *Complex Analysis*. Springer, July 2003.

[11] Themistocles M. Rassias and H. M. Srivastava. Some classes of infinite series associated with the riemann zeta and polygamma functions and generalized harmonic numbers. *Applied Mathematics and Computation*, 131(2-3):593–605, September 2002.

[12] Richard D. Mattuck. *A Guide to Feynman Diagrams in the Many-Body Problem*. Dover Publications, 2nd edition, June 1992.